Many-electron theory of x-ray photoelectron spectra: N-shell linewidths in the $_{46}$Pd to $_{92}$U range

Masahide Ohno* and Göran Wendin

Institute of Theoretical Physics, Chalmers University of Technology, S-412 96 Göteborg, Sweden

(Received 13 June 1984; revised manuscript received 29 November 1984)

The linewidths and energies of $4d$ holes (main lines in x-ray photoelectron spectra) are calculated for a number of elements in the range $_{70}$Yb to $_{92}$U, with use of nonrelativistic atomic many-body theory. The nonrelativistic Hartree-Fock frozen-core approximation for one-electron wave functions and Auger energies gives very good agreement with experiment. In the case of $4s$ and $4p$ holes, the Auger (in particular, super-Coster-Kronig) energies have to be calculated with inclusion of relaxation and relativistic effects. Combined with frozen-core, nonrelativistic one-electron wave functions, this gives good agreement with experimental energies and widths for $4s$ and $4p$ holes in $_{80}$Hg. In conclusion, it is very important to include the effects of two final-state holes on the Auger electron, as well as the polarization response which screens the Auger emission matrix element. This latter effect is largely equivalent to the so-called exchange interaction between the Auger electron and the final-state holes.

I. INTRODUCTION

X-ray photoelectron spectroscopy (XPS) is an important and direct method for studying the dynamics of relaxation and decay of core holes in atoms, molecules, and solids.[1] For example, the width of the photoelectron peaks gives the total decay of the corresponding hole level, and the intensity distribution over main lines and satellites gives information about the dynamics of the relaxation processes. Relaxation and decay are connected in a fundamental way through Kramers-Kronig relations involving the core-hole interaction energy:[1,2] The coupling between a core hole and the surrounding electronic charge density gives rise to a complex correction to the core-hole energy, the so-called self-energy, $\Sigma_i(E)$, which depends both on the orbital character and the energy of the core hole. The real part of the energy correction, $\mathrm{Re}\Sigma_i(E)$, describes the relaxation shift and the imaginary part, $\mathrm{Im}\Sigma_i(E)$, gives the damping (i denotes the hole; hole levels are underlined).

Experimentally, lifetime broadening of levels and satellite structure are directly observable manifestations of dynamic processes. Relaxation shifts can be deduced experimentally if the data are so complete that the entire satellite distribution of a core level is known, in which case the center of gravity of the intensity distribution gives the core-hole ionization energy in the absence of relaxation.[1] Usually, however, one has only information about the width and the binding energy of the core hole. In such cases, relaxation shifts have to be defined with the help of theoretical calculations.[1,2]

In order to judge the quality of theoretical calculations one has to compare theory with experiments for a number of core holes with different elements. This last point is particularly important: Variation of the atomic number implies variation of the kinetic energy of the Auger electrons as well as variation of the two-hole potential in which the Auger electron has to escape. This provides serious tests of theoretical models.

The calculations by McGuire[3] were the first ones to provide theoretical predictions of core-hole lifetimes due to nonradiative decay for a wide range of elements. These calculations were based on a golden-rule expression for the $\underline{i} \rightarrow jk\epsilon$ decay probability using Herman-Skillman type of wave functions

$$\Gamma_{\underline{i}} = 2\pi \sum_{j,k} | \langle i\epsilon | 1/r_{12} | jk \rangle |^2 . \qquad (1)$$

The results have been widely used and have been very useful for understanding the development of Auger spectra with atomic number, e.g., the opening and closing of decay channels. However, McGuire's[3] results have also become something of a standard reference, which is somewhat unfortunate since they represent an approximation which is *not generally valid*. For instance, Fuggle and Alvarado[4] have recently made an extensive comparison of experimental core-hole linewidths in the N shell with McGuire's calculations,[5] finding large differences for Coster-Kronig type of transitions. However, these problems are well known and well (but perhaps not widely) understood, even if nobody so far has been willing to go through the periodic system to produce tables that could replace the results by McGuire.[3,5] Nevertheless, there are results for selected core levels over extended ranges of the periodic system, showing good agreement with experiment (Refs. 1, 2, and 6—11).

For about 15 years it has been known that atomic photoionization cross sections in general cannot be described by one-electron models of Herman-Skillman (Hartree-Fock-Slater) type. The reason is that these models neglect the influence of the polarizability of the atomic shells.[12,13] The polarization effects can be incorporated in essentially three different but equivalent ways: through an effective transition matrix element, through an effective ionizing field, or in terms of an effective wave function for the emitted electron.[12,13] Naturally, this must also have

consequences for decay processes involving electron emission: Polarization effects have to be taken into account, either through an effective continuum wave function $|\epsilon\rangle_{\text{eff}}$,

$$\Gamma_i = 2\pi \sum_{j,k} |\langle i(\epsilon)_{\text{eff}}| 1/r_{12} |jk\rangle|^2 , \qquad (2)$$

or through dynamic screening of the Coulomb interaction which drives the decay,

$$\Gamma_i = 2\pi \sum_{j,k} |\langle i\epsilon| V(\mathbf{r}_1,\mathbf{r}_2;\omega) |jk\rangle|^2 . \qquad (3)$$

In Eq. (3), ω denotes the frequency of the internal perturbation, which is the same as the energy transfer from the core hole to the system, $\omega \simeq \epsilon_j - \epsilon_i$, leading to ionization (Auger emission). Moreover, the escaping Auger electron must feel the potential of two holes jk in the final state, and the kinetic energy (Auger energy) must be determined in a consistent manner (not necessarily the "best" experimental value).

The breakdown of one-electron approximations which neglect polarization can be understood more easily if we write Eq. (3) according to

$$\Gamma_i = 2\pi \sum_{j,k} |\langle \epsilon| \langle i| V(\mathbf{r}_1,\mathbf{r}_2;\omega) |j\rangle |k\rangle|^2 . \qquad (4)$$

When the initial (i) and final (j) orbitals in the core-hole transition belong to the same main shell, there is very large radial overlap and consequently the potential from the transition moment, $\langle i| V(\mathbf{r}_1,\mathbf{r}_2;\omega) |j\rangle$, can become very large. This is the characteristic of *Coster-Kronig transitions*: The internal perturbing potential is very strong, leading to large decay rates. Furthermore, if this perturbation ionizes the outermost (highest angular momentum) subshell of the same main shell, there will be two immediate consequences: First, the interaction strength will be very large [super-Coster-Kronig (sCK) transition, see Refs. 1—3 and 5—17] and second, the Auger energy will be low and the excitation energy will fall in a range where the polarizability is very large. This will lead to large corrections to the one-electron model, i.e., the effective Coulomb interaction $V(\mathbf{r}_1,\mathbf{r}_2;\omega)$ will be substantially different from the bare one $1/r_{12}$.

An interesting aspect is that very good agreement with experiment can be obtained for core-hole widths in solids for whole sequences of elements through the simple Herman-Skillman type of one-electron calculations (see Refs. 4—6 and 14). What matters is the overlap of the effective wave function in Eq. (2) with the core orbitals: Omission of polarization effects in the form of the repulsive electron-hole interaction and screening of the core hole can be compensated for by calculating the continuum Auger electron in the potential of a single initial hole and by adjusting Auger energies. Therefore, in such semiempirical calculations, good agreement with experiment does not imply that the intrinsic physical mechanisms are well understood.

II. GENERAL DISCUSSION OF N-SHELL CORE-HOLE LINEWIDTHS

A systematic treatment of the type described above was first applied by Wendin and Ohno[2] to N-shell ($4s,4p$) x-
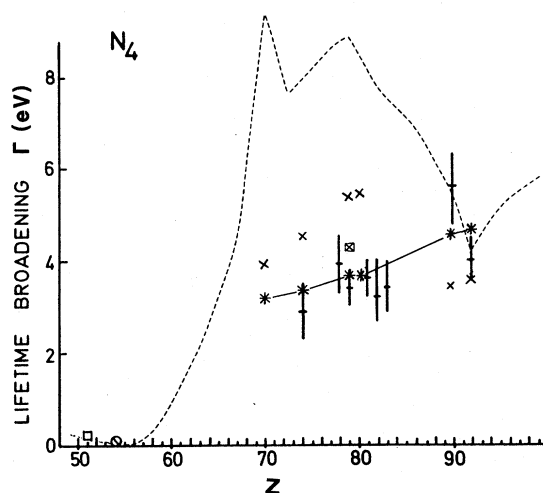

FIG. 1. Experimental and theoretical $4d_{3/2}$ linewidths of the elements in the range of $Z = 36$—90. The experimental results are those compiled by Fuggle and Alvarado (see Ref. 4 for explanation of notations in Fig. 1). Theory: *, present theory (A 1 approximation, frozen-core potential and frozen Auger energy); ×, present theory (A 2 approximation, frozen-core potential and relaxed and relativistic Auger energy); ⊠, present theory (A 3 approximation, relaxed-core potential and relaxed Auger energy); — — —, McGuire (Ref. 5).

ray photoelectron spectra [XPS, ESCA (electron spectroscopy for chemical analysis)] of $_{54}$Xe and then extended to a wider range of elements and core holes.[1,6—11,15—17]

Figures 1—5 show experimental N-shell linewidths (compilation by Fuggle and Alvarado[4]) together with the results of one-electron calculations by McGuire[15] and many-electron calculations by the present authors. The many-electron calculation results for the elements $_{70}$Yb—$_{92}$U are new, while the results in the range from $_{46}$Pd—$_{56}$Ba are taken from previous work.[1,2,9,10,18] McGuire's results are based on an approximate Herman-Skillman potential for the initial single-hole configuration, used for calculating bound and continuum orbital wave
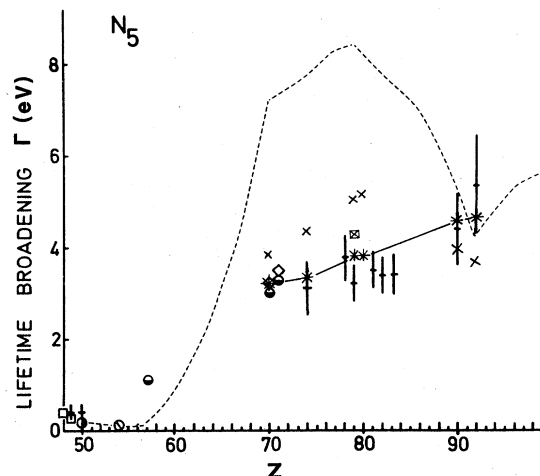

FIG. 2. Experimental and theoretical $4d_{5/2}$ linewidths of the elements in the range of $Z = 36$—90. Notation same as Fig. 1.
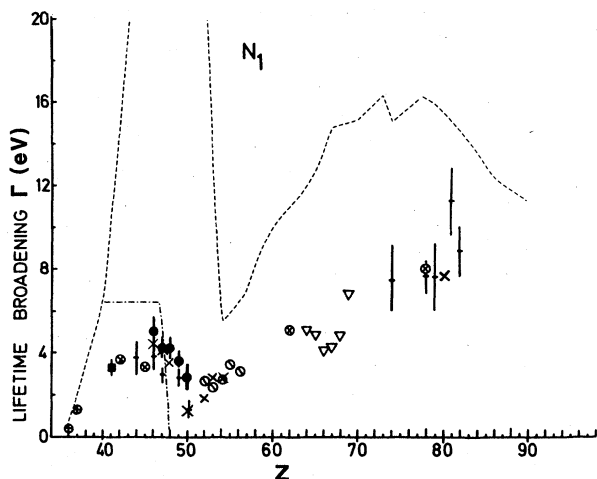
FIG. 3. Experimental and theoretical 4s linewidths of the elements in the range of $Z = 36-90$. The experimental results are those compiled by Fuggle and Alvarado (see Ref. 4 for explanation of notation). Theory: $\times$, present theory ($A\,2$ approximation, frozen-core potential, relaxed and relativistic Auger energy); $---$, McGuire (Ref. 5); $-\cdot-\cdot-\cdot$, McGuire (see Ref. 52).

functions. In the range of elements from $_{70}$Yb—$_{73}$Bi these one-electron linewidths are more than a factor of 2 larger than experiment, and the dependence upon atomic number does not seem to be correct if one includes the range up to $_{92}$U. Fuggle and Alvarado[4] suggested that this large discrepancy is due to the overestimate of N-NN (sCK) processes by McGuire.[5] This suggestion is confirmed by the present calculations, the results of which are in quite
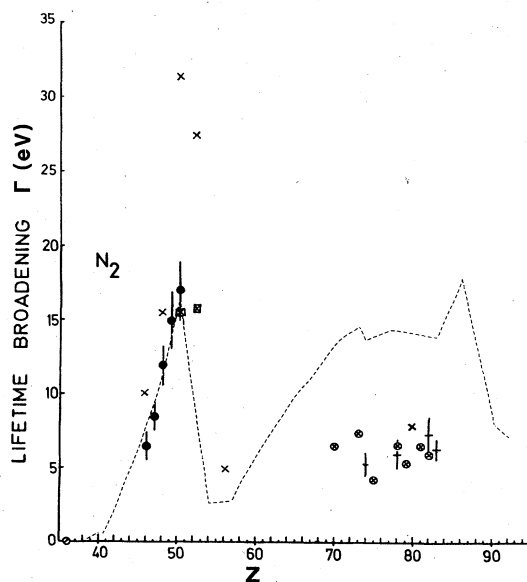

FIG. 4. Experimental and theoretical $4p_{1/2}$ linewidths of the elements in the range of $Z = 36-90$. The experimental results are those compiled by Fuggle and Alvarado (see Ref. 4 for explanation of notation). Theory: $\times$, present theory ($A\,2$ approximation); $\boxtimes$, present theory (relaxed orbital approximation, $A\,3$); $---$, McGuire (Ref. 5).
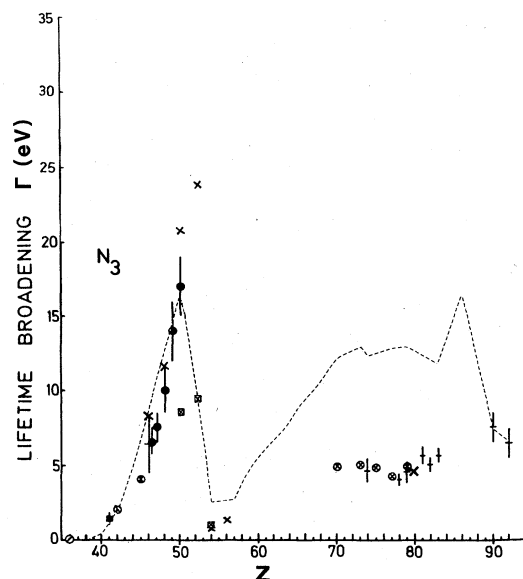

FIG. 5. Experimental and theoretical $4p_{3/2}$ linewidths of the elements in the range of $Z = 36-90$. Notation same as Fig. 4.

good agreement with experiment (Figs. 1 and 2; present theory represented by stars and crosses). However, we should like to emphasize that this type of behavior had already been extensively discussed and demonstrated in the completely analogous cases of M-MM super-Coster-Kronig transitions and M-shell linewidths in the elements $_{30}$Zn—$_{40}$Zr.[6-8,11,17] Moreover, the behavior of the 4s and 4p core-hole levels around $_{52}$Sn (Figs. 3—5) can be explained in similar terms, although there the general situation is a good deal more complicated.[1,9,10,18]

It should be noted that the relative strengths of the different decay processes can be directly determined from experimental Auger emission branching ratios. Experimental studies of the $4\underline{d} \rightarrow 4fX$ Coster-Kronig ($X = 5p, 5d$) and super-Coster-Kronig ($X = 4f$) types of Auger spectra for the elements $_{70}$Yb, $_{74}$W, $_{77}$Ir, $_{78}$Pt, $_{79}$Au, and $_{80}$Hg show that the calculated $4\underline{d} \rightarrow 4f^2/4\underline{d} \rightarrow 4f5\underline{d}$ branching ratio is very much overestimated by McGuire.[19-23]

As mentioned in the Introduction, not only the linewidth but also the relaxation energy shift of a core hole provides information about the dynamics and the interaction strength. A comparison of the experimental XPS hole energy (negative of the binding energy) of $_{80}$Hg with the Dirac-Fock ΔSCF hole energy (difference between the DF SCF total energy of the ground and ionic states), shows that the experimental peaks are shifted to lower binding energies by as much as ~ 9 eV for the $4\underline{s}$, $\sim 5-6$ eV for $4\underline{p}$, and ~ 3 eV for the $4\underline{d}$ levels.[24] These large discrepancies in hole energies of N levels of these high-Z elements demonstrate the importance of the super-Coster-Kronig mechanism for relaxation beyond ΔSCF (monopole relaxation). This kind of many-body effect has also been found in many core levels of the low- to intermediate-Z elements. Many-body calculations of XPS spectra of these core levels by the authors[1,2,6-13,18] have shown large improvements in comparison with the results calculated by McGuire[3,5,25] and Chen et al.[26] This is be-

cause of the consistent and systematic treatment of decay and relaxation processes by many-body theory, which provides the linewidth and relaxation energy shift at same time, includes polarization effects, and also provides a consistent choice of Auger energies.

In the present work we calculate the N-shell XPS spectra of the elements $_{70}$Yb, $_{74}$W, $_{79}$Au, $_{80}$Hg, $_{90}$Th, and $_{92}$U from first principles by using nonrelativistic diagrammatic atomic many-body theory. The results are in good and sometimes excellent agreement with experiment in what concerns both core-hole linewidths and binding energies. The present results show that the large discrepancy between the experiment and the results by McGuire[3,5,25] can be removed if the effects of the final-state double holes and the polarization response of the surrounding system are taken into account in a systematic way. In particular, the $4\underline{d}\leftrightarrow 4f^2\epsilon g$ super-Coster-Kronig process is no longer overestimated. The present results also imply that a large discrepancy in the $4s$ and $4p$ linewidths of these high-Z elements between McGuire's results[5] and experiment[4] can be removed in the same way, although these cases are somewhat delicate, as will be explained later on.

III. CORE-HOLE BINDING ENERGIES

In general the experimental atomic hole energy $E_{\underline{i}}$ (negative of the binding energy) can be approximated by

$$E_{\underline{i}} = E_{\underline{i}}(\Delta \text{SCF}) + \Delta_{\underline{i}}^p + \Delta_{\underline{i}}^C . \tag{5}$$

Here $E_{\underline{i}}(\Delta \text{SCF})$ is the atomic relativistic ΔSCF core-hole energy (this includes an energy shift due to static monopole relaxation), $\Delta_{\underline{i}}^p$ is the dipole relaxation shift (dominating contribution beyond monopole relaxation[1]), and $\Delta_{\underline{i}}^C$ is the ground-state correlation energy shift (see Refs. 1, 2, and 6—9 for detailed discussion). These quantities can be calculated from first principles. One of the main aims of the present work is to calculate the dipole relaxation shift of the N-shell hole levels in order to provide a good theoretical estimate of N-shell binding energies.

In Table I we list the differences between the atomic experimental and relativistic ΔSCF $4s$, $4p$, and $4d$ hole energies in the range from $_{70}$Yb—$_{93}$Np (Refs. 27—36). One should note the following points.

(i) For $4s$, $4p$, and $4d$ levels we obtain a large deviation from the ΔSCF hole energy. As will be shown in the present work, this energy shift is predominantly due to the dynamical dipolar $4\underline{s}\leftrightarrow 4\underline{p}4f\epsilon g$, $4\underline{p}\leftrightarrow 4\underline{d}4f\epsilon g$, and $4\underline{d}\leftrightarrow 4f^2\epsilon g$ virtual sCK processes.

(ii) For $4f$ levels the deviation is mainly due to the negative ground-state correlation shift $\Delta_{\underline{f}}^C$ which is neglected in the ΔSCF calculation. Note in particular the enormous correlation shift of $\Delta_{4f}^C \simeq -5$ eV in $_{70}$Y. We suggest that this is due to $4f \rightarrow 5d$ dipole-dipole ground-state correlation ($4f^2 \rightarrow 5d^2$ ground-state configuration interaction), which should be large due to low $4f^2$-pair excitation energies. With increasing atomic number Z, the $4f^2 \rightarrow 5d^2$ excitation energy rapidly increases and the $5d$ shell starts to fill up. As a consequence, as we see it, the $4f$ correlation energy falls rapidly and stabilizes around $\Delta_{4f}^C \simeq -2-2.5$ eV (Table I). However, as seen in Table I, for $Z > 80$ an anomaly appears in the $4f$ level shift. According to Wendin,[1] the $4f$ and $5\underline{p}_{1/2}5\underline{d}$ levels become degenerate around $Z = 83$, follow each other until $Z = 92$, and then separate. We therefore propose that the true ground-state $4f$ correlation shift remains approximately constant, ~ -2 eV, in the region around $_{90}$Th: The deviation is most likely due to configuration interaction through the virtual $4f \leftrightarrow 5\underline{p}5\underline{d}6\underline{d}, \epsilon d$ Auger process.

(iii) We assume that the ground-state correlation shift of the $4\underline{s}$, $4\underline{p}$, and $4\underline{d}$ levels is approximately the same as that of the $4f$ level, although the detailed correlation mechanism must be different for different levels in the case of $_{70}$Yb. The dynamic dipolar relaxation shifts $\Delta_{\underline{i}}^p$ should then be about 2 eV larger than the deviations listed in Table I in the range from $_{73}$Ta to $_{93}$Np. Note that also the $4\underline{p}$ and $4\underline{d}$ (and probably $4\underline{s}$) level shifts peak around $_{90}$Th (Table I), which probably reflects the influence of the collapsed $6d$ orbitals on the virtual Coster-Kronig and Auger processes.

(iv) The Auger energy is 6.8 and 5.4 eV higher than predicted by Dirac-Fock ΔSCF calculation for the

TABLE I. Differences between the experimental and relativistic atomic ΔSCF $4s$, $4p$, $4d$, and $4f$ hole energy of the elements $_{70}$Yb—$_{93}$Np (eV).

Element	$4s$	$4p_{1/2}$	$4p_{3/2}$	$4d_{3/2}$	$4d_{5/2}$	$4f_{5/2}$	$4f_{7/2}$
$_{70}$Yb		0.0	0.0	−0.6	−0.9		−5.0
$_{73}$Ta	5.2	3.4	2.7	0.6	0.7	−2.7	−2.6
$_{74}$W	6.2	5.6	4.2	1.5	1.7	−2.0	−1.9
$_{75}$Re	6.5	5.1	4.0	1.8	1.9	−2.0	−1.8
$_{76}$Os	6.5	4.5	4.2	1.7	2.0	−2.1	−2.0
$_{78}$Pt	5.9	5.0	4.0	1.5	1.7	−2.7	−2.6
$_{79}$Au	6.7	5.7	4.3	2.0	2.0	−2.6	−2.6
$_{80}$Hg	8.7	6.1	4.9	2.9	2.9	−2.3	−2.3
$_{81}$Tl	8.2	6.0	5.2	3.0	2.8	−1.9	−1.7
$_{82}$Pb	8.7	7.6	5.5	4.0	3.6	−1.0	−1.2
$_{83}$Bi	8.9	8.2	5.2	3.8	3.6	−1.1	−1.1
$_{90}$Th		6.1	5.2	4.7		1.1	1.2
$_{92}$U		8.0	5.1	3.7	3.1	−0.3	−0.6
$_{93}$Np		9.5	5.6	2.6	2.2	−0.1	−0.9

$4\underline{d}\rightarrow 4\underline{fX}$ ($X=4f$, $5p$, and $5d$) (s)CK spectra of $_{70}$Yb and $_{80}$Hg, respectively.[22,23] These Auger energy shifts are due to the ground-state correlation energy shift of the initial and final hole state and the dynamical relaxation energy shift of the initial hole.

We can expect similar energy shifts in x-ray emission energies when the initial- or the final-state hole, or both, involve this kind of dynamical relaxation processes. From this viewpoint one of the authors[37,38] has recently analyzed the L-x-ray emission energy of intermediate-Z elements measured by Putila-Mäntylä et al.[37] and the K,L-x-ray emission energy of intermediate- to high-Z elements measured by Kessler et al.[39]

IV. $4d$ XPS SPECTRA OF Yb—U

A. Spectral function and self-energy

Within the framework of a sudden approximation the XPS core-hole spectrum can be well approximated by the spectral function of the initial core hole given by[1,2]

$$A_{\underline{i}}(E)=\frac{1}{\pi}\frac{\mathrm{Im}\Sigma_{\underline{i}}(E)}{[E-E_{\underline{i}}^0-\mathrm{Re}\Sigma_{\underline{i}}(E)]^2+[\mathrm{Im}\Sigma_{\underline{i}}(E)]^2}, \quad (6)$$

where the self-energy $\Sigma_{\underline{i}}(E)$ is given by

$$\Sigma_{\underline{i}}(E)=\sum_{j,k}\sum_{L,S}\int d\epsilon\,\frac{|V_{i\epsilon jk}^{LS}(E)|^2}{\epsilon-E_{jk}^{LS}+E-i\delta} \quad (7)$$

with real and imaginary parts

$$\mathrm{Re}\Sigma_{\underline{i}}(E)=\sum_{j,k}\sum_{L,S}\int d\epsilon\,\mathrm{P}\frac{|V_{i\epsilon jk}^{LS}(E)|^2}{\epsilon-E_{jk}^{LS}+E}, \quad (8)$$

$$\mathrm{Im}\Sigma_{\underline{i}}(E)=\pi\sum_{j,k}\sum_{L,S}|V_{i\epsilon jk}^{LS}(E)|^2. \quad (9)$$

The excitation matrix element $V_{i\epsilon jk}^{LS}(E)$ accounts for polarization, relaxation, and ground-state correlation effects on the process in question, which can be described in typically two ways, as discussed in the Introduction,

$$V_{i\epsilon jk}^{LS}(E)=\langle i\epsilon\,|\,V(\mathbf{r}_1,\mathbf{r}_2;E)\,|\,jk(LS)\rangle \quad (10a)$$

$$=\langle i(\epsilon)_{\mathrm{eff}}\,|\,1/r_{12}\,|\,jk(LS)\rangle. \quad (10b)$$

By using the spectral function approach we obtain a consistent description of the line shift and lifetime broadening of the core-hole spectrum in terms of the self-energy. When this self-energy varies slowly in the neighborhood of a resonance at $E=E_p$, the spectral function can be approximated by

$$A_{\underline{i}}=\frac{1}{\pi}\frac{\Gamma_p/2}{(E-E_p)^2+(\Gamma_p/2)^2} \quad (11)$$

with the width Γ_p

$$\Gamma_p=2Z_p\mathrm{Im}\Sigma_{\underline{i}}(E), \quad (12)$$

$$Z_p=\left[1-\frac{\partial}{\partial E}\mathrm{Re}\Sigma_{\underline{i}}(E)\right]_{E=E_p}^{-1}. \quad (13)$$

Here Z_p is the residue at the pole, showing how much of

the original unit strength of the unperturbed hole remains at the pole. Z_p thus gives the relative strength of the line at $E=E_p$ in the core-hole spectrum, i.e., in the XPS spectrum (neglecting photoionization matrix elements).

Equation (11) is valid only when the self-energy varies slowly over the width [Eq. (12)] of the resonance. This situation applies to the present work, where we calculate the spectral function of a $4d$ hole in the elements $_{70}$Y—$_{92}$U. However, since Z_p [Eq. (13)] is typically 0.97, the result for the linewidth is essentially the same as directly using Eqs. (2) or (3) when calculating linewidths (provided one knows the correct energy for evaluation of the matrix element). Note, however, that Eq. (11) can not be used for describing $4\underline{p}$ (and in some cases $4\underline{s}$) spectra in the range $Z=50$ to Z approaching 70 due to the extremely strong $4\underline{p}\leftrightarrow 4\underline{d}^24f,\epsilon f$ and $4\underline{s}\leftrightarrow 4\underline{p}4\underline{d}4f,\epsilon f$ giant Coster-Kronig processes.[1,2]

B. Calculation of the self-energy; frozen and relaxed basis sets

The $4\underline{d}\leftrightarrow 4\underline{fX}$ ($X=5s$, $5p$, $5d$, and $4f$) (s)CK processes dominate the decay processes of a $4\underline{d}$ hole. Therefore, in the present work we consider only these processes when calculating the $4d$ self-energy. The method of evaluating the self-energy has been described in detail in previous papers[1,2,6–9] and here we only summarize the basic features of the zeroth-order orbital basis we use.

1. Frozen-core approximation (A1,A2)

(i) For hole levels we use Hartree-Fock (HF) orbitals of the neutral atom (average configuration).

(ii) For particle levels we use continuum orbitals calculated in a frozen HF V^{N-2} potential constructed using the neutral-atom ground-state HF orbitals with two holes in the final ionic state (average configuration). For the $4f\epsilon g$ ionic excitation channel electron-hole pair excitations are treated within the random-phase approximation with exchange (RPAE) accomplished by calculating the excited continuum g state according to

$$(4\underline{f})_{\mathrm{av}}(4\underline{f}\epsilon g\;^1P)\text{ frozen HF }V^{N-2}\text{ potential} \quad (14)$$

and adding Fermi-sea correlation. Equation (11) describes the ionic excitation as $(4\underline{f}\epsilon g)$ dipole excitation in a spherically averaged ionic system with a $4f$ hole. This level of approximation becomes essential when polarization effects become important as in the present $4\underline{d}\leftrightarrow 4\underline{f}^2\epsilon g$ sCK process.

The two-hole final state is the correct final state for an atomic system. In a metal the situation is more complicated since the final-state holes will be screened out and may also propagate away if they are located in conduction bands. If the Auger electron leaves the system with low energy, then the time scale for emission may be comparable to the time scales for screening or delocalization and a proper dynamical treatment becomes necessary. In most cases, however, the Auger (sCK) electrons are fast and a frozen-core approximation for the two-hole potential becomes relevant. We shall return to this point below.

Using the frozen-core approximation for the basis set

leads to a consistent approximation corresponding to a well-defined diagrammatic many-body expansion. By this expansion we can describe the dynamics of the primary photoionization process and the emission processes within a one-step model,[8,10] which also permits us to include effects of interference between the excitation and emission steps.[12] By this scheme, the relaxation and shake-up effects should be included via the corresponding diagrams describing the levels shifts, screened interactions, and multiple excitations.[1,2,9–13]

(iii) Auger energy parameters: In the calculation of the self-energy and the spectral function (linewidth) of a hole, the choice of Auger energy parameters must be consistent with the choice of basis set. The present frozen-core approximation neglects completely the effects of monopole relaxation and relativistic effects on the wave functions of the particle and hole states. Therefore, for a consistent choice we must calculate the Auger energy parameter as the difference between the frozen-core ionization energies (Koopmans's energies) for single and double holes

$$\epsilon_A = \begin{cases} E_{jk} - E_i & \text{(general)} \tag{15a} \\ E_j^0 + E_k^0 - F^0(j;k) - E_i^0 & \text{(frozen core) .} \tag{15b} \end{cases}$$

Here E_i^0, E_j^0, and E_k^0 are nonrelativistic Hartree-Fock one-electron energies and $F^0(j;k)$ is the bare Coulomb repulsion between the holes j and k in the frozen ground-state charge distribution. By this choice we exclude monopole relaxation and relativistic effects both from the wave functions and the excitation energies, so that the Auger energies become consistent with the choice of basis set. We name this *approximation A1*.

As the next step, we introduce the monopole relaxation energy shift and the relativistic energy shifts for single- and double-hole levels.[40] This choice of energy parameter corresponds to the use of the *experimental atomic Auger energy*. We name this *approximation A2*. This approximation has been successful for the calculation of the XPS spectra of the L, M, and N levels of low- to intermediate-Z elements. However, the approximation is not fully consistent in the sense that the monopole relaxation and relativistic effects are included only in terms of the initial single-hole and final double-hole level shifts while the corresponding effects on the wave functions are neglected.

2. Relaxed orbitals approximation (A3)

We have also examined, in the case of a single element, $_{79}$Au, an approximation where monopole relaxation is taken into account in the continuum wave function of the Auger electron as well as in the single-hole and two-hole energies. The basis set has the following characteristics.

(i) Hole levels; HF ground-state orbitals relaxed in the presence of one $4d$ core level.

(ii) Particle levels; orbitals calculated in a HF V^{N-2} potential constructed using orbitals from the double-hole HF ionic ground state (i.e., relaxed two-hole level). In particular, for the sCK channel

$(4f)_{\text{av}}(4\underline{f}\epsilon g\,^1P)$ HF $V^{N-2}(4\underline{f}^2)$ relaxed potential   (16)

RPAE is employed, as in the frozen-core approximation to calculate the $4d$ self-energy and the decay probability.

(iii) Auger energy parameter: As we assume that the escaping Auger electron will see the potential of the fully relaxed final double holes, in order to be consistent we use the nonrelativistic HF ΔSCF hole energies for the initial single-hole and final double-hole energies.

The need for consistency can be seen in the following manner: The core-hole linewidth can be regarded as a function of the Auger energy[8] [Eqs. (1)–(3)], $\Gamma_i(\epsilon)$, and the shape of this function depends on the two-hole potential. Especially in the case of super-Coster-Kronig processes $\Gamma_i(\epsilon)$ may vary rapidly in the region of the actual Auger energy and a consistent choice of ϵ becomes essential. Starting from the unrelaxed case, relaxation effects will have two major effects. First, the two-hole—one-electron (e.g., $4f^2\epsilon g$) continuum threshold will relax more than the single-hole level (e.g., $4\underline{d}$) (about 4 times as much) so that the Auger energy will increase. This leads to an increase in core-hole linewidth because $\Gamma_i(\epsilon)$ increases with ϵ in this region (delayed onset due to slowly penetrating ϵg wave). Second, relaxation will make the two-hole potential less attractive in the core region so that the linewidth function $\Gamma_i(\epsilon)$ rises more slowly. This will lower the core-hole linewidth at the frozen-core kinetic energy, which energy therefore has to be raised in order to give the same overlap with the core orbitals as in the frozen-core case (the core orbitals change very little due to relaxation). This raise of the Auger energy was, however, already provided by the same relaxation process: There is now self-consistency. As long as the Auger energy is reasonably large, the frozen and relaxed approaches should give similar core level widths. However, when the Auger energy tends towards zero, the relaxed approach is the only possible one. We shall refer to this approximation as the *A3 approximation*.

V. $4d$ HOLE: RESULTS AND DISCUSSION

A. $4d$ hole energy

In Table II we list the $4d$ hole energy calculated by the $A1$ (frozen-core potential, frozen Auger energy) and $A2$ (frozen-core potential, relaxed relativistic Auger energy) approximations. In the case of the $A2$ approximation the hole energy corresponds to the solution of Dyson's equation, i.e., we evaluate Eq. (6) in the case that E_i^0 is a relativistic ΔSCF energy and the self-energy $\Sigma_i(E)$ includes Coster-Kronig and super-Coster-Kronig processes which give rise to the dipole relaxation shift. In the case of the $A1$ approximation Eq. (6) is evaluated with E_i^0 as a Hartree-Fock Koopmans's energy, and resulting dipole relaxation shift is added to the unperturbed Dirac-Hartree-Slater or Dirac-Hartree-Fock ΔSCF hole energy. The experimental atomic hole energies listed in Table II are those obtained in Sec. II, except for $_{80}$Hg which is taken from Ref. 33.

The calculated $4d$ hole energies are in general about ~ 1–2 eV less than the experimental ones because of neglect of the ground-state correlation energy shift dis-

TABLE II. Experimental and theoretical $4d$ hole energy of the elements $_{70}$Yb—$_{90}$Th (eV). Note that ΔSCF energy for $_{80}$Hg is from Ref. 24.

Element	Expt.	$4d_{3/2}$ Theory				Expt.	$4d_{5/2}$ Theory			
		$A\,1$	$A\,2$	ΔSCF[a]	DF[b]		$A\,1$	$A\,2$	ΔSCF[a]	DF[b]
$_{70}$Yb	-199.0	-196.0	-196.1	-198.4	-211.7	-190.1	-186.8	-186.9	-189.2	-202.0
$_{74}$W	-265.2	-264.1	-264.1	-267.0	-280.7	-252.7	-251.0	-250.9	-253.9	-267.6
$_{79}$Au	-360.8	-359.6	-359.1	-362.6	-377.3	-342.7	-341.4	-341.0	-344.4	-358.4
$_{80}$Hg	-385.4	-385.2	-384.7	-388.3	-402.6	-366.0	-365.8	-365.4	-368.9	-382.4
$_{90}$Th	-721.7	-724.6	-723.0	-726.9	-743.5	-684.5	-686.9	-685.9	-689.2	-704.8

[a]Reference 36.
[b]Reference 35.

cussed in Sec. II. The calculated $4d$-hole dipole relaxation energy shift is about 3 eV for the elements of present interest. This energy shift is caused primarily by the virtual $4\underline{d}\leftrightarrow 4f^2\epsilon g$ sCK process.

B. $4d$ linewidth

In Figs. 1 and 2 and in Table III we show the present theoretical linewidths, the results by McGuire,[5] and the experimental widths obtained by XPS AES (Auger-electron spectroscopy), and XES (x-ray emission spectroscopy). In Table IV we list the present theoretical partial decay width ratios, the results by McGuire[5] and the experimental ones obtained by AES. One should note the following points.

(i) The total linewidths calculated by the present theory give generally better or much better agreement with experiment than other theoretical calculations. In particular, the $A\,1$ approximation gives much better agreement with the XPS data than approximation $A\,2$ in the Yb-U region, which we ascribe to the fact that the $A\,1$ approximation represents a consistent scheme. As pointed out in Sec. IV, the $A\,2$ approximation is not consistent, because the Auger energy is too high in relation to the potential seen by the Auger electron. The result of the relaxed-orbitals approximation for $_{79}$Au for the $4\underline{d}_{5/2}$ linewidth is 4.4 eV in comparison to 3.8 eV from the $A\,1$ approximation. This difference is fairly small because the Auger energy is large, in which case both of the approximations should work reasonably well and give similar results.

The development of the linewidth with relaxation can be seen for $_{79}$Au in Fig. 1: In comparison with the all-frozen $A\,1$ approximation with $\Gamma_{4d}=3.8$ eV, using atomic relativistic ΔSCF $4\underline{d}$ and $4f^2$ energies increases the Auger energy and raises the width of the $4d$ hole to 5.3 eV. Relaxation of the $4f^2\,V^{N-2}$ potential seen by the continuum g electrons [Eq. (15)] ($A\,3$) finally lowers the $4\underline{d}$ width to 4.4 eV. Even this $A\,3$ approximation is not fully consistent, since the wave function of the initial $4d$ hole has not been relaxed. However, it is not clear what is the most reliable approximation using statically relaxed ionic configurations.[8] Since the linewidth is fairly sensitive to relaxation effects, short of more careful dynamical calculations the relaxed result for the $4\underline{d}$ level of $_{79}$Au in Figs. 1 and 2 can be regarded as a reasonable estimate of the importance of relaxation. However, we do not know for in-

stance whether a correct treatment of relaxation should bring us back down to the value of 3.8 eV for the width of the $4\underline{d}_{5/2}$ hole from the $A\,1$ approximation: This value agrees better with experiment.

(ii) In order to examine the importance of polarization effects in the $4\underline{d}\leftrightarrow 4f^2\epsilon g$ sCK process, we compare the partial decay width by this decay channel for Au in the frozen HF V^{N-2} (average configuration, one-electron approximation; no polarization effects), the Tamm-Dancoff approximation with exchange (polarization effects in the final state) and RPAE (polarization effects in the final and initial states).[1,2] The results are 2.13, 1.14, and 1.00 eV, respectively, which shows that it is *very important to take into account the polarization* of the surrounding system in response to the electron-hole excitation.

(iii) McGuire[5] evaluated the linewidths using the wave functions generated by the approximate Herman-Skillman Hartree-Fock-Slater (HFS) potential of the initial single-hole configuration for both initial and final bound states and the continuum wave function calculated in the approximate HFS V^{N-1} potential of singly ionized initial configuration. This approximation already includes the effects of relaxation in the presence of the initial single hole in contrast to the present frozen-core approximation. However, the exchange term in the HF configuration average potential as well as the Slater exchange term in the HFS calculation describe the average potential of the bound electrons and do not account for the repulsive exchange interaction between the hole and the continuum electron. The potential is therefore more attractive than the potential obtained from the *LS*-dependent HF scheme,[8,12,13,41,42] and this was also recognized by McGuire[16] and Chen *et al.*[17] As a consequence, the CK and sCK transition rates will generally be overestimated for low Auger energies and underestimated for sufficiently high Auger energies if one uses potentials which do not incorporate polarization effects.[8] The present results show the importance of simultaneously taking into account the effects of the proper electron-hole exchange interaction (polarization) and the V^{N-2} ionic potential from the localized double vacancy in the final state on the Auger electron.[43] Finally, it should be noted that for the $4f\rightarrow\epsilon g$ excitation channel we have also taken into account ground-state correlations within the random-phase approximation with exchange.[1,2]

(iv) The experimental $4\underline{d}$ linewidths of $_{90}$Th and $_{92}$U

TABLE III. Theoretical and experimental $4d$ linewidths of the elements $_{70}$Yb—$_{92}$U (eV).

Element	$4d_{3/2}$						$4d_{5/2}$				
		Expt.		Theory				Expt.	Theory		
	XPS	AES	XES	Present		McGuire	XPS	AES	Present		McGuire
				$A\,1$	$A\,2$				$A\,1$	$A\,2$	
$_{70}$Yb	5.41[a]	4.2[b]	5.25 ±0.96[c]	3.18	4.02	9.35	3.3[e]	4.2[b]	3.18	3.87	7.24
			5.24 ±1.20[d]				5.41[a]				
$_{74}$W	3.0 ±0.6[e]	5.0 ±0.7[f]	4.45 ±0.93[c]	3.41	4.61	7.89	3.2 ±0.6[e]	5.0 ±0.7[f]	3.41	4.39	7.72
			5.38 ±1.02[d]								
			5.58[g]								
			4.48[h]								
			8.46 ±0.72[i]								
$_{79}$Au	3.5 ±0.3[e]		5.1[j] 5.3[k]	3.76	5.33	8.83	3.3 ±0.3[e]		3.76	5.09	8.4
$_{80}$Hg	4.3[l] 4.4[m]		4.0 ±0.5[n]	3.76	5.37		4.0[l] 4.0[m]	4.0 ±0.5[n]	3.76	5.22	
$_{90}$Th	5.7 ±0.9[e]			4.63	3.49	5.27	4.5 ±0.8[e]		4.63	3.90	5.25
$_{98}$U	4.0 ±0.4[e]			4.69	3.61	4.23	5.4 ±1.1[e]		4.69	3.73	4.17

[a]Reference 53.
[b]Reference 22.
[c]Reference 47, from L_3-N_4 x-ray emission width.
[d]Reference 47 from L_2-N_4 x-ray emission width.
[e]Reference 4.
[f]Reference 20.
[g]Reference 45.
[h]Reference 46.
[i]Reference 48.
[j]Reference 54 from L_2-N_4 x-ray emission width.
[k]Reference 54 from L_3-N_4 x-ray emission width.
[l]Reference 33 (atom).
[m]Reference 33 (solid).
[n]Reference 23, McGuire's results are from Ref. 5.

metal (Figs. 1 and 2) show large variations between the $J = \frac{5}{2}$ and $\frac{3}{2}$ levels as well as between the elements. This is understandable, however: The Th—U region is complicated since the $4d$-hole energy is nearly degenerate with the $4f^2$ and $4f5\underline{s}$ thresholds and, moreover, the $6d$ orbitals have collapsed and start to become occupied. With increasing atomic number, this will lead to the closing of previously open decay channels, and this may happen differently for different spin-orbit levels due to the large spin-orbit splitting. In addition, the threshold condition may lead to satellite structure, e.g., $4f^26d$ stealing intensity from $4\underline{d}$. Finally, whether channels are open or closed may depend on whether one considers the free atom or the metal. In the atomic, all-frozen, $A\,1$ approximation the thresholds and the Auger energies are not correctly

described, and the $4\underline{d}$-$4f^2$ super-Coster-Kronig decay processes are forbidden. Nevertheless, the $A\,1$ approximation seems to give a very good average value in Th—U region (Figs. 1 and 2) for the $4\underline{d}$ total linewidth. Note that in this case (closed sCK channels) our $4\underline{d}$ linewidths agree quite well with McGuire's results.[5]

From a physical point of view, in this case the $A\,2$ approximation should be more realistic (the best would be $A\,2$ with relaxation, $A\,3$, which we have not investigated). In *atomic* Th, the $4\underline{d}_{5/2}$-$4f^2$ *and* the $4\underline{d}_{3/2}$-$4f^2$ *sCK decay channels are closed* while the CK channels are open. This *atomic* result is shown in Figs. 1 and 2, and the linewidth difference between the N_5 and N_4 levels ($N_5 > N_4$) is due to the large spin-orbit splitting. In Th *metal*, taking into account the atom-solid Auger energy shift calculated by

TABLE IV. Theoretical and experimental partial decay width ratios. Experimental data for Au are from Ref. 21 (upper value) and Ref. 19 (below) and for Hg from Ref. 23. The value in parentheses for Au is the value obtained by assuming mean free path proportional to $E^{1/2}$ (kinetic energy). The value in parentheses for Hg is for polynomial background. McGuire's results are quoted in Ref. 21.

Element	$4d_{3/2}$ $\dfrac{\Gamma_{N_4-N_{6,7}O_{4,5}}}{\Gamma_{N_4-N_{6,7}}}$ Theory A1	A2	McGuire	Expt.	$\dfrac{\Gamma_{N_4-N_{6,7}N_{6,7}}}{\Gamma_{\text{total}}}$ Theory A1	A2	McGuire	Expt.	$4d_{5/2}$ $\dfrac{\Gamma_{N_5-N_{6,7}O_{4,5}}}{\Gamma_{N_5-N_{6,7}N_{6,7}}}$ Theory A1	A2	McGuire	Expt.	$\dfrac{\Gamma_{N_5-N_{6,7}N_{6,7}}}{\Gamma_{\text{total}}}$ Theory A1	A2	McGuire
$_{70}$Yb					0.79	0.84							0.79	0.82	
$_{74}$W	4.40	8.58	4.06		0.60	0.74			4.40	7.16	4.06		0.60	0.70	
$_{79}$Au	0.66	2.36		1.5(1.9) 0.14	0.28	0.58	0.65	0.54 0.12	0.66	1.72		1.5(1.9) 0.14	0.28	0.50	0.65
$_{80}$Hg	0.46	2.07	3.33	0.71(0.88)	0.22	0.56	0.61	0.38(0.43)	0.46	1.49	3.33	0.38(0.43)	0.22	0.46	0.61

Mårtensson et al.[44] we find that the N_4 sCK decay channel opens up, which should increase the N_4 width about 1 eV. We suggest that the experimental N_4-N_5 difference of about 1 eV ($N_4 > N_5$) is due to the closing of the N_5 sCK decay channel in $_{92}$Th. We also conclude that with the present approximations we cannot get entirely satisfactory agreement with experiment.

In *atomic* U, the $N_{4,5}$ sCK decay channels are both closed and, in addition, the $4\underline{d}_{5/2}-4f5\underline{s}$ CK decay channel is closed. In Figs. 1 and 2, this explains why the theoretical value for the N_5 width, in the $A2$ approximation, drops and becomes nearly equal to the N_4 width. However, in U *metal* the $4\underline{d}_{5/2}$-$4f5\underline{s}$ CK decay channel is *open*, which should increase the N_5 width by 0.5 eV. The agreement with experiment is then reasonable already in the $A2$ approximation.

For Th, in Table II we see that the calculated energy shift ($A2$ approximation) is somewhat too low to agree with experiment: If we add a ground-state correlation shift of, say, -2 eV, we need an additional shift of about $+3$ eV in order to get agreement with experiment. This is very similar to the anomaly in the $4f$ line shift in Th. Possibly, the additional $4\underline{d}$ shift might come from the $4\underline{d}$-$4\underline{f}^2 6d$ interaction process, which we have neglected in the present calculation. The configurations are nearly degenerate, and the effects might be significant.

(v) We should comment on the experimental linewidths listed in Table III. In the case of XES measurements we derive the $4d$ linewidths by subtracting the $L_{2,3}$ linewidths calculated by Chen et al.[26] from the experimental XES linewidths.[45-48] The recent L-level x-ray absorption spectrum of $_{80}$Hg measured by Keski-Rahkonen et al.[47] shows that the linewidths calculated by Chen et al.[26] agree very well with the experimental data for the $L_{2,3}$ levels. However, the theoretical result is larger than the experimental one by a factor of 2 for the L_1 level due to overestimate of the L_1-$L_3M_{4,5}$ sCK processes. A similar large discrepancy for the L linewidth of the elements $_{41}$Nb—$_{50}$Sn has been already pointed out by Putila-Mäntylä et al.[50] A large discrepancy for the L linewidth of the elements $_{29}$Cu—$_{32}$Ge has been discussed by one of the authors recently.[12] The $4d$ linewidths derived from the L_{γ_1} (L_2-N_4) x-ray emission width measured by Gokhale et al.[48] is much larger than the results by the others. L_{α_1} (L_3-M_5), L_{α_2}(L_3-M_4), and L_{β_1} (L_2-M_4) linewidths measured by these authors are in excellent agreement with the theoretical results by Chen et al.[26] and other experimental measurements.[45-47] The theoretical linewidths by Chen et al.[26] give good agreement with the experiment for the $L_{2,3}$ and $M_{4,5}$ levels because these levels do not involve strong CK and sCK decay processes. Note that the L_1 level of the high-Z elements is shifted about 8 eV from the relativistic hole energy by the L_1-L_3M_4 CK virtual processes.[49,51] This is also the case for the low- to intermediate-Z elements.[12,37,51]

VI. $4s$-$4p$ XPS SPECTRA

A. The medium-Z region

Figures 3—5 show two distinct regions, namely $Z \sim 40$—56 and $Z \sim 60$—90. Although the calculations by

McGuire,[5] and also (not shown) by Chen et al.,[52] seem to do well in the range $Z \sim 40$—54 region, in our opinion this good agreement is fortuitous: The physical polarization effects are neglected and this is compensated for by the choice of core potentials and Auger energies. Moreover, the linewidths are so large that the perturbation scheme [Eq. (1)] actually breaks down (this was realized by Chen et al.[52]) and one has to start from Eq. (6). In the $Z = 40$—54 region we are dealing with particularly strong giant Coster-Kronig processes, $4p \leftrightarrow 4\underline{d}^2 \epsilon f$ and $4\underline{s} \leftrightarrow 4\underline{p} 4\underline{d} \epsilon f$. These problems have been treated in some detail by Wendin and Ohno[1,2,9,10] and the results for $4\underline{s}$ and $4p$ linewidths are shown in Figs. 3—5. In the light of the present work, one might have obtained good linewidth results with the all-frozen (A 1) approximation, but we have not checked this possibility. The $N_{2,3}$ linewidths for $_{50}$Sn in Figs. 3 and 4, however, clearly demonstrate the necessity for consistent approximation: Inclusion of polarization effects and a two-hole final-state potential have to be combined with inclusion of relaxation effects (A 3 approximation).

B. The high-Z region, in particular $_{80}$Hg

In the high-Z region, $Z \sim 60$—90, the situation is completely different: The previously mentioned giant Coster-Kronig processes are forbidden and replaced by the weaker sCK processes, especially $4\underline{s} \leftrightarrow 4\underline{p} 4\underline{f} \epsilon g$ and $4p \leftrightarrow 4\underline{d} 4\underline{f} \epsilon g$. Now perturbation theory applies but oddly enough, in this region McGuire's[5] results dramatically overestimate the N-shell linewidths and do not reproduce the experimental Z dependence. However, systematic application of the same many-electron methods[1,2,9,10] that have good results in the $Z = 40$—56 region now also gives satisfactory agreement in the high-Z region. We have only checked this for mercury, $_{80}$Hg, but we are convinced that this result applies to the whole range of elements. This means in particular that by taking into account polarization (electron-hole exchange) effects and by using a physical two-hole final-state ionic potential, one obtains immediately a reasonable description of the super-Coster-Kronig decay rates. It also means that the present scheme works quite well using nonrelativistic one-electron wave functions even in the case of $4\underline{s}$ and $4p$ levels.

In $_{80}$Hg, the $4\underline{s}$ and $4p$ hole energies are shifted from the relativistic ΔSCF energies by as much as 9 and 6 eV, respectively (see Table I). In the present work we have calculated the $4\underline{s}$ and $4\underline{p}$ XPS spectra of Hg by nonrela-

tivistic many-body theory for the core-hole spectral function, as already described in Sec. IV. However, in contrast to the $4\underline{d}$ case, in the case of $4\underline{s}$ and $4p$ holes the A 1 approximation becomes useless because it leads to the closing of very important super-Coster-Kronig decay processes which are physically allowed. Therefore, in the present work we have calculated the $4\underline{s}$ and $4p$ hole spectra of Hg within the framework of the A 2 approximation, using frozen-core continuum wave functions but relaxed and relativistic hole energies. With this approximation we can expect to have a reasonable estimate of the widths and positions of the $4\underline{s}$ and $4p$ core holes, but we should not expect the A 2 approximation to give accurate linewidths. The energies, on the other hand, should be fairly accurate since the energy shift is rather insensitive to the approximation [integral over the excitation spectrum, Eq. (8)].

The calculated $4\underline{s}$ and $4p$ hole energies and widths are listed in Table V (see also Figs. 3—5) together with the experimental data by Svensson et al.[33] Somewhat surprisingly, the results are in quite good agreement with experiment. In analogy with the $4\underline{d}$ case, one would have expected the A 2 approximation to give widths too large, to be corrected by including relaxation effects on the continuum wave functions (approximation A 3). The good result of the A 2 approximation could result from compensating errors, not having treated relativistic effects on the wave functions, or it could be the result of a coincidence for $_{80}$Hg. This problem could be resolved by studying a range of elements, as in the $4\underline{d}$ case, but unfortunately we have not had the opportunity to do this yet.

The dipole relaxation shifts of the $4\underline{s}$ and $4p$ levels are predominantly due to virtual $4\underline{s} \leftrightarrow 4\underline{p} 4\underline{f} \epsilon g$ and $4p \leftrightarrow 4\underline{d} 4\underline{f} \epsilon g$ sCK processes, and are quite insensitive to the detailed description of these channels: However, note that the use of HF ^1P wave functions exaggerates the shift (related to the fact that the oscillator-strength sum rule is not fulfilled) and that one has to work within the RPAE to have a consistent description.[1,2,8] The above-mentioned sCK channels are closed in the A 1 approximation because the hole-hole interaction in the double vacancies is unscreened and very large, so that the two-hole levels move to more negative energies than the single-hole levels. This would not influence the energy shift in any serious way but the effect on the linewidth would be catastrophic.

In conclusion, the large difference between the results by McGuire[5] and experiment is caused by the same reasons as in the $4\underline{d}$ case, primarily omission of polarization (electron-hole exchange) effects and, to some extent,

TABLE V. Theoretical and experimental $4s$ and $4p$ hole energy and linewidth of $_{80}$Hg (eV).

Level	Hole energy			Linewidth		
	Expt.[a]	Theory		Expt.[a]	Theory	
		Present	ΔSCF[b]		Present	McGuire[c]
$4s$	-809.4	-810.7	-818.1	9.8	7.75	14.6
$4p_{1/2}$	-687.4	-687.9	-693.5	8.6	7.87	14.0
$4p_{3/2}$	-583.8	-583.6	-588.7	5.0	4.40	12.8

[a]Reference 33.
[b]Reference 24.
[c]Interpolation by Svensson et al. (Ref. 33) for $_{77}$Ir, $_{79}$Au, and $_{83}$Bi from Ref. 5.

inappropriate final-state potential and Auger energies. Finally, let us mention that our calculated $[(4\underline{s}\text{-}4\underline{p}4f)/\text{total}]$ partial decay ratio is 0.1 and the $[(4\underline{p}\text{-}4\underline{d}4f)/\text{total}]$ partial decay ratios for the $4\underline{p}_{1/2}$ and $4\underline{p}_{3/2}$ hole levels are 0.8 and 0.32, respectively.

VII. AUGER SPECTRA

The core-hole self-energy $\Sigma_i(E)$ in Eq. (7) contains, by construction, information about the branching of the Auger decay processes onto all different final states. However, since $\Sigma_i(E)$ is integrated over these final states, as a consequence $\text{Im}\Sigma_i(E)$ only leads to the *total* decay width, as shown in Eq. (12). The *partial* decay widths are obtained by explicitly calculating the transition probabilities to the different final states describing Auger emission. A one-step treatment of the photoionization-Auger emission process then gives the result for the Auger current $I_A(\epsilon;\omega)$ (Refs. 8 and 10):

$$I_A(\epsilon;\omega)$$
$$\sim \sum_i \int dE \, |\langle i \,|\, r\cos\theta \,|\, \epsilon+E\rangle|^2$$
$$\times A_i(E) \sum_{j,k}\sum_{L,S} \frac{\pi\,|V_{i\epsilon jk}(E)|^2}{\text{Im}\Sigma_i(E)} \delta(\epsilon - E_{\underline{jk}}^{LS} + E) \ . \tag{17}$$

This result is not fully general since we have assumed the final double vacancy to be sharp and structureless (no broadening, no satellite structure). The simplest type of generalization would be to broaden the final state by introducing a term-level-dependent width $\Gamma_{\underline{jk}}^{LS}$:

$$\delta(\epsilon - E_{\underline{jk}}^{LS} + E) \rightarrow A_{\underline{jk}}^{LS}(\epsilon + E)$$

$$= \frac{1}{\pi} \frac{\Gamma_{\underline{jk}}^{LS}/2}{(\epsilon - E_{\underline{jk}}^{LS} + E)^2 + (\Gamma_{\underline{jk}}^{LS}/2)^2} \ . \tag{18}$$

The super-Coster-Kronig processes only influence, in the present case, the initial core hole through the self-energy $\Sigma_i(E)$, leading to the line-shape function $A_i(E)$. The self-energy $\Sigma_i(E)$ is integrated over all continuum energies and summed over all hole configurations jk and associated term levels LS. The spectral function $A_i(E)$ is therefore quite insensitive to the final-state term-level structure, unless the core level $\underline{i}$ happens to be degenerate with the LS structure of a particular $\underline{jk}$ final-state double vacancy.

Assuming constant dipole matrix element and a single Lorentzian core hole with $\Gamma_{\underline{i}} \gg \Gamma_{\underline{jk}}^{LS}$, Eq. (17) reduces to

$$I_A(\epsilon;\omega) \sim \int dE \frac{\Gamma_{\underline{i}}/2}{(E - E_{\underline{i}})^2 + (\Gamma_{\underline{i}}/2)^2}$$
$$\times \sum_{j,k}\sum_{L,S} \frac{\Gamma_{i\epsilon jk}^{LS}}{\Gamma_{\underline{i}}} \delta(\epsilon - E_{\underline{jk}}^{LS} + E) \ . \tag{19}$$

The super-Coster-Kronig process dominates the core-hole energy shift $\Delta_{\underline{i}}^P = \text{Re}\Sigma_{\underline{i}}(E_{\underline{i}})$. However, the width $\Gamma_{\underline{i}} \cong 2\,\text{Im}\Sigma_{\underline{i}}(E_{\underline{i}})$ is determined by both the sCK and CK processes, and to some small extent the Auger processes.

The sCK process does not dominate nearly as dramatically as in the McGuire calculations,[5] as can be seen in Table IV.

Finally, since the branching ratios vary slowly over the core-hole width, we may perform the energy integration in Eq. (19), obtaining[10]

$$I_A(\epsilon;\omega) \sim \sum_{j,k}\sum_{L,S} \frac{\Gamma_{i\epsilon jk}^{LS}}{\Gamma_{\underline{i}}} \frac{\Gamma_{\underline{i}}/2}{(E_{\underline{jk}}^{LS} - E_{\underline{i}} - \epsilon)^2 + (\Gamma_{\underline{i}}/2)^2} \ . \tag{20}$$

In reality, however, we perform our calculations in the LS-averaged approximation, with the result

$$I_A(\epsilon;\omega) \sim \sum_{j,k} \frac{\Gamma_{i\epsilon jk}}{\Gamma_{\underline{i}}} \frac{\Gamma_{\underline{i}}/2}{(E_{\underline{jk}} - E_{\underline{i}} - \epsilon)^2 + (\Gamma_{\underline{i}}/2)^2} \ , \tag{21}$$

where

$$\Gamma_{i\epsilon jk} = \sum_{L,S} \Gamma_{i\epsilon jk}^{LS} \ . \tag{22}$$

This partial width, and the associated branching ratio $\Gamma_{i\epsilon jk}/\Gamma_{\underline{i}}$, is to be compared with the corresponding quantities from Eq. (20) which are obtained by integration over the Auger energy ϵ for each $\underline{jk}$ configuration, and which directly correspond to the experimentally deduced branching ratios (see Table IV for the case of $i = 4\underline{d}$).

The virtual super-Coster-Kronig process strongly screens the partial widths $\Gamma_{i\epsilon jk}$ and dramatically reduces both the sCK partial width and the sCK/CK branching ratio (Table IV) in comparison with McGuire[5] (note, however, that a large part of this reduction is also connected with a *consistent choice of Auger energy*). Since the sCK/CK and sCK/total branching ratios involve a summation over term levels, they automatically become insensitive to the term-level dependence of the super-Coster-Kronig process. On the other hand, there must be some effects, which we have not investigated, of LS dependence on the LS-split coupled sCK emission channels. This would influence the relative intensities of the term levels within each of the $4f^2(4\underline{d}\text{-}4f^2\epsilon g)$, $4\underline{d}4f(4\underline{p}\text{-}4\underline{d}4f\epsilon g)$, and $4\underline{p}4\underline{d}(4\underline{s}\text{-}4\underline{p}4f\epsilon g)$ final-state configurations. Furthermore, the virtual sCK process will screen the CK and Auger processes (intershell interaction), which will mainly influence the sCK/CK branching ratios somewhat.

In Table IV we present numerical results for the sCK/CK and sCK/total branching ratios in the case of a $4d$ core hole. As could be expected, the branching ratios are very sensitive tests of the different choices of approximations. However, the present approximations give much better agreement with experiment than the other theoretical results. As pointed out by Aksela and Aksela,[23] the contradictory experimental results of Larkins and Lubenfeld[19] and Matthew et al.[21] for the partial decay width ratio of solid Au is possibly due to the difficulties associated with the background subtraction and the variations of the spectrometer transmission. Aksela and Aksela[23] also pointed out that a large difference (a factor of 2) in the partial decay width ratios between the results by Matthew et al.[21] for solid $_{79}$Au and the results by Aksela and Aksela[23] for vapor $_{80}$Hg probably comes from different behavior of the spectrometer collection efficiencies in the

lower kinetic energy range. They conclude that their spectrometer should give a good intensity ratio for Hg. As there should not be a large difference in decay ratios between Au and Hg, we should compare the present theoretical results for Au with the experimental data for Hg. Matthew et al.[21] studied experimentally the variation of the $4\underline{d}\rightarrow4f5\underline{d}/4\underline{d}\rightarrow4f^2$ decay width ratio with the number of $5\underline{d}$ electrons. For $_{74}$W Rawlings et al.[20] observed that $4\underline{d}\rightarrow4f5\underline{d}$ transitions are very weak. The experimental and theoretical results show that ratio increases more sharply than linear in the number of $5d$ electrons in contrast to the linear variation suggested by a simple theory along the lines of Allen et al.[55]

VIII. SUMMARY AND CONCLUDING REMARKS

The purpose of the present work has been to show that McGuire's[5] calculations of lifetime widths for N-shell holes can relatively easily be corrected by inclusion of polarization effects (electron-hole exchange effects) in the final state. The resulting $4\underline{s}$, $4\underline{p}$, and $4\underline{d}$ core-hole widths are in fair to good agreement with experiment, leaving no serious discrepancies to be explained, in the range of elements from $_{70}$Y to $_{92}$U.

The calculations are based on the spectral function and the self-energy for a core hole, calculated within the RPAE and taking into account the two-hole final-state ionic potential when calculating one-electron wave functions for the Auger electrons. We are particularly interested in *consistent approximations*, where the Auger energy is consistent with the one-electron potential seen by the Auger electron. The simplest approximation, which also gives best agreement with experiment in the $4\underline{d}$ case, is a nonrelativistic frozen-core approximation for both hole energies and wave functions. This approximation works well from $_{70}$Y up to $_{92}$U (for $_{90}$Th and $_{92}$U in an average sense). However, in reality, relaxed and relativistic hole energies have to be employed for $4\underline{d}$ holes in $_{90}$Th and $_{92}$U and for $4\underline{s}$ and $4\underline{p}$ holes in $_{70}$Yb—$_{92}$U. Somewhat to our surprise, this works fairly well for the linewidths (and even better for energy shifts) although we use nonrelativistic frozen-core one-electron wave functions. We have, however, calculated too few cases to be able to judge whether the good agreement for the linewidths of $4s$ and $4p$ holes in $_{80}$Hg is systematic or coincidental.

Our investigation shows that it is essential to include the effects of the localized, final-state double vacancy on the Auger electron also in the metals. The transition probabilities are determined in the core region inside the metallic screening radius and are therefore atomiclike. Atomic models give a good description of core-hole energy shifts and widths due to Coster-Kronig and super-Coster-Kronig processes also for the metals, with some deviations in critical cases where the atom-to-solid shift causes a closed decay channel to open up. An example of this might be the $4\underline{d}$ levels in $_{90}$Th and $_{92}$U.

*Present address: Physikalisches Institut der Universität Bonn, D-5300 Bonn 1, Federal Republic of Germany.
[1]G. Wendin, *Structure and Bonding* (Springer, Berlin, 1981), Vol. 45, p. 1 and references therein.
[2]G. Wendin and M. Ohno, Phys. Scr. **14**, 148 (1976).
[3]E. J. McGuire, in *Atomic Inner-Shell Processes*, edited by B. Crasemann (Academic, New York, 1975), Vol. 1, p. 293.
[4]J. C. Fuggle and S. F. Alvarado, Phys. Rev. A **22**, 1615 (1980).
[5]E. J. McGuire, Phys. Rev. A **9**, 1840 (1974), and references therein.
[6]M. Ohno and G. Wendin, Solid State Commun. **24**, 75 (1977).
[7]M. Ohno and G. Wendin, J. Phys. B **11**, 1557 (1978).
[8]M. Ohno and G. Wendin, J. Phys. B **12**, 1305 (1979).
[9]M. Ohno, Phys. Scr. **21**, 589 (1980); J. Phys. C **13**, 447 (1980).
[10]M. Ohno and G. Wendin, Solid State Commun. **39**, 875 (1981).
[11]M. Ohno, J. Phys. B **17**, 195 (1984); Phys. Rev. B **29**, 3127 (1984).
[12]G. Wendin, in *New Trends in Atomic Physics*, Les Houches Summer School, Session XXXVIII, 1982, edited by G. Grynberg and R. Stora (Elsevier, New York, 1984), p. 555.
[13]G. Wendin, in *X-ray and Atomic Inner-Shell Physics—1982*, *(International Conference, University of Oregon)*, Proceedings of the International Conference on X-ray and Atomic Inner-Shell Physics, edited by B. Crasemann (AIP, New York, 1982), p. 495.
[14]L. I. Yin, I. Adler, T. Tsang, M. H. Chen, D. A. Ringers, and B. Crasemann, Phys. Rev. A **9**, 1070 (1974).
[15]McGuire (Ref. 16) and Chen et al. (Ref. 17) have also included effects of polarization in the case of the $3\underline{p}\leftrightarrow3\underline{d}^2\epsilon f$ sCK transition in $_{29}$Cu (Ref. 16) and $_{30}$Zn (Ref. 17), by calculating effective continuum wave functions which take into account the exchange interaction between the emitted electron and the final-state holes [Eq. (2)].
[16]E. J. McGuire, Phys. Rev. A **16**, 2365 (1977).
[17]M. H. Chen, B. Crasemann, M. Aoyagi, and H. Mark, Phys. Rev. A **18**, 802 (1978).
[18]M. Ohno, P. Putila-Mäntylä, and G. Graeffe, J. Phys. B **17**, 1747 (1984).
[19]F. P. Larkins and A. Lubenfeld, J. Electron Spectrosc. **12**, 111 (1977).
[20]K. J. Rawlings, B. J. Hopkins, and S. D. Foulias, J. Electron Spectrosc. **18**, 213 (1980).
[21]J. A. Matthew, F. P. Netzer, and E. Bertel, J. Electron Spectrosc. **20**, 1 (1980).
[22]I. Chorkendorff, J. Onsgaard, H. Aksela, and S. Aksela, Phys. Rev. B **27**, 945 (1982).
[23]H. Aksela and S. Aksela, J. Phys. B **16**, 1531 (1983).
[24]J. F. McGilp and P. Weightman, J. Phys. B **13**, 1953 (1980).
[25]E. J. McGuire, Phys. Rev. A **5**, 1043 (1972), and references therein.
[26]M. H. Chen, B. Crasemann, and H. Mark, Phys. Rev. A **24**, 177 (1981), and references therein.
[27]The experimental atomic data are obtained by using the atom-solid energy shift calculated by Johansson and

Mårtensson (Ref. 28) and the solid-state data complied by Nyholm *et al.* (Ref. 29) for $_{73}$Ta—$_{92}$U and by Kowalczyk (Ref. 30) for $_{70}$Yb. For $_{93}$Np, N hole energies are obtained from those of NpO$_2$ measured by Krause *et al.* (Ref. 31) by taking into account the metal-oxide energy shift (~ 3 eV) estimated from the case of $_{92}$U (see Ref. 32). For $_{80}$Hg we use the experimental atomic XPS data by Svensson *et al.* (Ref. 33). The atom-solid energy shift which is fairly level independent is found to be 7.4 eV for $_{80}$Hg, while the experimental atom-solid energy shift of N levels in $_{80}$Hg are ~ 6.4—7.2 eV. For the theoretical relativistic atomic ΔSCF hole energies we use the following data: For $_{80}$Hg we use the Dirac-Fock ΔSCF energies calculated by McGilp and Weightman (Ref. 24) and for $_{92}$U and $_{93}$Np the Dirac-Fock ΔSCF hole energies by Carlson and Nestor (Ref. 34). For the other elements we obtained the DF ΔSCF hole energies approximately by obtaining the monopole relaxation shift approximately from the DF eigenvalues calculated by Desclaux (Ref. 35) and Dirac-Hartree-Fock-Slater ΔSCF hole energies by Huang *et al.* (Ref. 36). We have only used the ΔSCF results by Huang *et al.* (Ref. 36) for closed-shell atoms (elements $_{70}$Yb, $_{80}$Hg, and $_{86}$Rn) and interpolated the monopole relaxation for the surrounding elements, because the spin-orbit splitting calculated with their method is inaccurate for open-shell atoms in the range of interest here. The values listed in Table I should not be taken too literally because the error occurred in the data treatment can be as much as ~ 0.5 eV.

[28]B. Johansson and N. Mårtensson, Phys. Rev. B **21**, 4427 (1980).

[29]R. Nyholm, A. Berndtsson, and N. Mårtensson, Uppsala University Report No. UUIP-1031 (1980) (unpublished).

[30]S. P. Kowalczyk, Ph.D. thesis (Lawrence Berkeley Laboratory Report No. LBL-4319) University of California, Berkeley, 1976 (unpublished).

[31]M. O. Krause, C. W. Nestor, Jr., and J. H. Oliver, Phys. Rev. A **15**, 2335 (1977).

[32]J. C. Fuggle, A. F. Burr, L. M. Watson, D. J. Fabian, and W. Lang, J. Phys. F **4**, 335 (1974).

[33]S. Svensson, N. Mårtensson, E. Basilier, P. Å. Malmquist, U. Gelius, and K. Siegbahn, J. Electron Spectrosc. **9**, 51 (1976).

[34]T. A. Carlson and C. W. Nestor, Jr., At. Data Nucl. Data Tables **19**, 153 (1977).

[35]J. P. Desclaux, At. Data Nucl. Data Tables **12**, 311 (1973).

[36]K-N. Huang, M. Aoyagi, M. H. Chen, B. Crasemann, and H. Mark, At. Data Nucl. Data Tables **18**, 243 (1976).

[37]P. Putila-Mäntylä, M. Ohno, and G. Graeffe, J. Phys. B **16**, 3503 (1983).

[38]M. Ohno, Phys. Rev. A **30**, 1128 (1984).

[39]E. G. Kessler, Jr., R. D. Deslattes, D. Girard, W. Schwitz, L. Jacobs, and O. Renner, Phys. Rev. A **26**, 2696 (1982).

[40]We use the relativistic Dirac-Hartree-Fock-Slater (Ref. 36) or Dirac-Hartree-Fock (Ref. 24) ΔSCF energies for the initial hole E_I^0. For the final-state double-hole energies, we employ the non-relativistic HF ΔSCF method (average configuration). We then introduce the average relativistic energy shift of the final double holes as a sum of a single-hole shifts, which we obtain from the Dirac-Fock and HF eigenvalues of single holes. The calculated relativistic average double-hole energies are in good agreement with the experimental ones for atomic $_{70}$Yb and $_{80}$Hg (Refs. 22 and 23).

[41]J. E. Hansen, J. Phys. B **5**, 1083 (1972).

[42]G. Wendin and A. F. Starace, J. Phys. B **11**, 4119 (1978), and references therein.

[43]In the work by Chen *et al.* (Ref. 17) the CK electron was coupled to proper LS term levels of the double-hole core. Such an approach neglects the coupling between different CK continuum channel based on different double-hole LS levels. The remaining interchannel interaction will have significant effects and might be the reason why the result of Chen *et al.* (Ref. 17) for the $3p$ level width in $_{30}$Zn is not as good as that of Ohno and Wendin (Ref. 8). In the approach of Ref. 8, the double-hole LS structure is not resolved (not introduced) and the interchannel interaction therefore automatically accounted for. This is also the approach of the present paper.

[44]N. Mårtensson, P. Hedegård, and B. Johansson, Phys. Scr. **29**, 154 (1984).

[45]J. H. Williams, Phys. Rev. **45**, 71 (1934).

[46]J. N. Cooper, Phys. Rev. **61**, 2341 (1942); **65**, 155 (1944).

[47]S. I. Salem and P. L. Lee, Phys. Rev. A **10**, 2033 (1974).

[48]B. G. Gokhale, S. N. Shukla, and R. N. Srivastava, Phys. Rev. A **28**, 858 (1983).

[49]O. Keski-Rahkonen, G. Materlik, B. Sonntag, and J. Tulkki, J. Phys. B **17**, L121 (1984).

[50]P. Putila-Mäntylä, M. Ohno, and G. Graeffe, J. Phys. B **17**, 1735 (1984).

[51]M. H. Chen, B. Crasemann, and H. Mark, Phys. Rev. A **24**, 1158 (1981).

[52]M. H. Chen, B. Crasemann, L. I. Yin, T. Tsang, and I. Adler, Phys. Rev. A **13**, 1435 (1976).

[53]C. S. Fadley and D. A. Shirely, Phys. Rev. A **2**, 1109 (1970).

[54]F. K. Richtmyer, S. W. Barnes, and E. Ramberg, Phys. Rev. **46**, 843 (1934).

[55]G. C. Allen, P. M. Tucker, and R. K. Wild, Surf. Sci. **68**, 469 (1977).